IMPLEMENTATION OF THE CMS-EXO-17-015 ANALYSIS IN THE MADANALYSIS 5 FRAMEWORK

BENJAMIN FUKS

Laboratoire de Physique Théorique et Hautes Energies (LPTHE), UMR 7589, Sorbonne Université et CNRS, 4 place Jussieu, 75252 Paris Cedex 05, France

Institut Universitaire de France, 103 boulevard Saint-Michel, 75005 Paris, France

ADIL JUEID

Department of Physics, Konkuk University, Seoul 05029, Republic of Korea

We present an implementation of the CMS-EXO-17-015 analysis in the MadAnalysis 5 framework. The analysis targets a search for dark matter in a channel in which it originates from the production and decay of a pair of scalar leptoquarks. This search considers a luminosity $\mathcal{L} = 77.4$ fb^{-1} of CMS data collected in 2016 and 2017, in proton-proton collisions at a centre-of-mass energy of 13 TeV. The final state signature is comprised of one isolated highly-energetic muon, one jet with a large transverse momentum and a significant amount of missing transverse energy. We validate our re-implementation in MadAnalysis 5 for a specific leptoquark/dark matter benchmark scenario. In particular, we compare predictions obtained with MadAnalysis 5 with the official CMS results for various kinematical distributions relevant for the CMS-EXO-17-015 analysis, as well as detailed cut-flow tables. We have found an excellent agreement.

1. Introduction

Since the discovery of the Higgs boson, the Standard Model (SM) of particle physics is considered to be a good low energy approximation of a more complete, yet undiscovered, theoretical framework. Such a theoretical framework may in particular be able to address questions such as the nature of dark matter (DM) in the universe, among many other interesting issues. Unfortunately, only little is known about the true nature of DM, despite the extensive searches carried out both in laboratories and astrophysical experiments.

At the LHC, one of the most known of and used strategies consists of looking for the presence of a significant excess in the tail of the missing transverse energy ($|\vec{p}_{\rm miss}|$) distribution. A specific emphasis is put on a signature comprised of dark matter particles recoiling against a visible hard SM object like a photon, a jet, an electroweak gauge boson or even an SM Higgs boson or a top quark [1–8]. Multiple associated searches have been conducted by the ATLAS and the CMS collaborations, the most recent ones analysing data recorded during the LHC Run 2 [9–31]. Consequently to the absence of direct evidence for the existence of DM so far, these results have been used to severely constrain the DM couplings and masses in large

classes of new physics scenarios. In particular, the absence of any DM signal at the LHC in the so-called thermal freeze-out mechanism has called for either going beyond standard freeze-out, or investigating alternative models.

One of the most attractive of those contexts is the so-called co-annihilation paradigm in which DM is produced in association with beyond-the-SM partners very close in mass. In the framework developed in Ref. [32], the SM field content is extended by a scalar leptoquark doublet M_s, a weak doublet of Dirac fermions X and a Majorana fermion χ that plays the role of dark matter. These new states have the following assignments under the SM gauge group $SU(3)_c \otimes SU(2)_L \otimes U(1)_Y$,

$$M_s \equiv \begin{pmatrix} M_s^u \\ M_s^d \end{pmatrix} : (\mathbf{3}, \mathbf{2}, 7/3) \qquad X \equiv \begin{pmatrix} X_u \\ X_d \end{pmatrix} : (\mathbf{3}, \mathbf{2}, 7/3), \qquad \chi : (\mathbf{1}, \mathbf{1}, 0), \tag{1}$$

and the relevant interaction Lagrangian $\mathcal{L}_{\rm NP}$ can be written as

$$\mathcal{L}_{\rm NP} = -\left(y_D \overline{X} M_s \chi + y_{Q\ell} \overline{Q}_L M_s \ell_R + y_{Lu} \overline{L}_L M_s^c u_R + \text{h.c.}\right). \tag{2}$$

In parallel, the LHC collaborations developed search strategies dedicated to this class of models. The CMS-EXO-17-015 analysis [33] considered in this proceedings contribution is one of these. In this analysis, the CMS collaboration has focused on one of the benchmarks detailed in Ref. [32]. It assumes that $y_{Lu} = 0$, and the other model parameters are chosen as

$$y_{Q\ell} = \sqrt{2}/10, \; y_D = 0.1, \; \text{and} \; \; \Delta = \frac{M_X - m_\chi}{m_\chi} = 0.1. \tag{3}$$

In this note, we report on the implementation of this CMS-EXO-17-015 analysis in the MadAnalysis 5 framework [34–38]. The relevant code for the MadAnalysis 5 implementation can be found in https://doi.org/10.14428/DVN/ICOXG9. In Sec. 2, we describe the analysis that we re-implemented, including a detailed description of the object definitions and event selection strategy. We discuss the validation of our re-implementation, focusing both on the Monte Carlo event generation necessary for this task and on a comparison of the MadAnalysis 5 predictions with the official CMS results, in Sec. 3. We summarise our work in Sec. 4.

2. Description of the analysis

In the considered theoretical framework, leptoquark (LQ) pair production and decay lead to several signatures, their respective relevance depending on the LQ branching ratios. In the CMS-EXO-17-015 analysis, the final state under consideration is comprised of one isolated muon, one jet and a large amount of missing transverse energy. This process is illustrated by the Feynman diagram shown in Fig. 1.

2.1. *Object definitions*

As above-mentioned, the considered analysis relies on the presence of hard final-state jets and muons, as well as on the one of a large amount of missing transverse

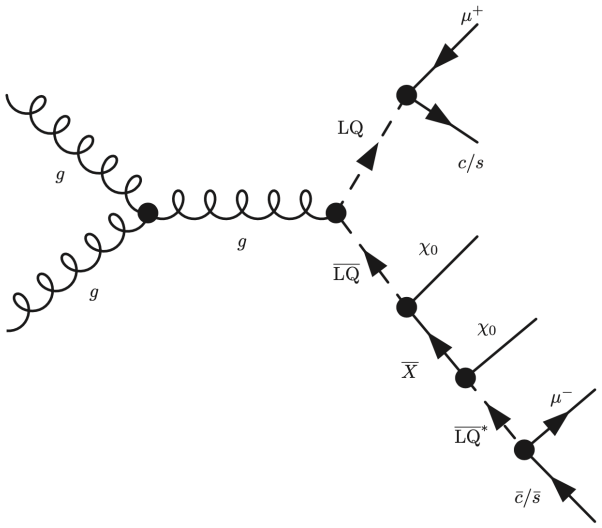

Fig. 1. Representative parton-level Feynman diagram illustrating the class of processes probed by the CMS-EXO-17-015 analysis.

energy. In addition, a veto is imposed on the presence of final-state objects of a different nature.

Candidate muons (the leading one being assumed to originate from the decay of a LQ, as illustrated by the Feynman diagram of Fig. 1) are required to satisfy tight selection criteria [39]. Moreover, their transverse momentum p_T^μ and pseudorapidity η^μ must fulfil

$$p_T^\mu > 60 \text{ GeV}, \text{ and } |\eta^\mu| < 2.4. \tag{4}$$

In addition, those muons are enforced to be isolated to suppress any potential contribution of muons arising from hadronic decays. This relies on an isolation variable I defined by

$$I \equiv \frac{1}{p_T^\mu} \sum_i p_{T,i}, \tag{5}$$

with the sum running over all photon, neutral hadron and charged hadron candidates reconstructed within a distance, in the transverse plane, of $\Delta R \equiv \sqrt{(\Delta\eta)^2 + (\Delta\phi)^2} = 0.4$ around the muon direction. This isolation variable is required to satisfy $I < 0.15$. On the other hand, the analysis also makes use of *loose muons* to reduce the contribution of Z+jets background events (see below). Those are required to satisfy $I < 0.25$ and $p_T^\mu > 10$ GeV.

Reconstructed electron candidates are required to have a transverse momentum $p_T^e > 15$ GeV and a pseudorapidity $|\eta^e| < 2.5$. Moreover, they are considered only if they satisfy loose identification criteria [40]. Hadronically decaying tau leptons (τ_h) are also identify through loose criteria [41], their selection additionally enforcing $p_T^\tau > 20$ GeV and $|\eta^\tau| < 2.3$.

Jets are reconstructed by means of the anti-k_T algorithm [42], with a radius parameter $R = 0.4$[a]. The signal jet collection is then comprised of all jets whose pseudorapidity satisfies $|\eta^j| < 2.4$. The Combined Secondary Vertex (CSVv2) algorithm is then used to identify the jets originating from the fragmentation of a b-quark, the analysis making use of its tight working point [43]. The corresponding b-tagging efficiency is given by

$$\mathcal{E}_{b|b}(p_T) = \begin{cases} -0.033 + 0.0225\ p_T - 3.5{\cdot}10^{-4}\ p_T^2 + 2.586{\cdot}10^{-6}\ p_T^3 - 9.096{\cdot}10^{-9}\ p_T^4 \\ \quad +1.212{\cdot}10^{-11}\ p_T^5 \qquad \text{for } \ 20\ \text{GeV} < p_T \leqslant 50\ \text{GeV}\ , \\ 0.169 + 0.013\ p_T - 1.9{\cdot}10^{-4}\ p_T^2 + 1.373{\cdot}10^{-6}\ p_T^3 - 4.923{\cdot}10^{-9}\ p_T^4 \\ \quad +6.87{\cdot}10^{-12}\ p_T^5 \qquad \text{for } \ 50\ \text{GeV} < p_T \leqslant 160\ \text{GeV}\ , \\ 0.62 - 8.3{\cdot}10^{-4}\ p_T + 4.3078{\cdot}10^{-7}\ p_T^2 \\ \quad \text{for } \ 160\ \text{GeV} < p_T \leqslant 1000\ \text{GeV}, \end{cases} \tag{6}$$

while the associated mistagging probabilities of a charmed jet ($\mathcal{E}_{c|b}$) and a light jet ($\mathcal{E}_{j|b}$) as a b-jet are given by

$$\mathcal{E}_{c|b}(p_T) = \begin{cases} 0.0234 - 8.417{\cdot}10^{-5}\ p_T + 1.24{\cdot}10^{-6}\ p_T^2 - 5.5{\cdot}10^{-9}\ p_T^3 + 9.96{\cdot}10^{-12}\ p_T^4 \\ -6.32{\cdot}10^{-15}\ p_T^5 \qquad \text{for } \ 20\ \text{GeV} < p_T \leqslant 65\ \text{GeV}\ , \\ 0.0218 + 2.46{\cdot}10^{-5}\ p_T - 2.021{\cdot}10^{-8}\ p_T^2 \\ \quad \text{for } \ 65\ \text{GeV} < p_T \leqslant 1000\ \text{GeV}, \end{cases}$$

$$\mathcal{E}_{j|b}(p_T) = \begin{cases} 0.00284 - 8.63{\cdot}10^{-5}\ p_T + 1.38{\cdot}10^{-6}\ p_T^2 - 9.69{\cdot}10^{-9}\ p_T^3 + 3.19{\cdot}10^{-11}\ p_T^4 \\ -3.97{\cdot}10^{-14}\ p_T^5 \qquad \text{for } \ 20\ \text{GeV} < p_T \leqslant 150\ \text{GeV}, \\ 6.3{\cdot}10^{-4} + 4.51{\cdot}10^{-6}\ p_T + 2.83{\cdot}10^{-9}\ p_T^2 \\ \quad \text{for } 150\ \text{GeV} < p_T \leqslant 1000\ \text{GeV}. \end{cases} \tag{7}$$

Finally, one defines the missing transverse energy as the magnitude of the transverse momentum imbalance ($\vec{p}_{\text{miss}}$), which is computed as the opposite of the vec-

[a]In the CMS-EXO-17-015 search, jet clustering excludes the charged-particle tracks that are not associated with the primary interaction vertex. This is irrelevant for our reimplementation as we neglect any potential pile-up effects.

torial sum of the transverse momentum of all reconstructed objects,

$$\vec{p}_{\rm miss} = -\left[\sum_{\rm electrons} \vec{p}_T + \sum_{\rm muons} \vec{p}_T + \sum_{\rm photons} \vec{p}_T + \sum_{\rm hadrons} \vec{p}_T\right].$$

In our simulation setup, we have implemented the above parametrisations in a customized Delphes 3 card that has then been used for the simulation of the CMS detector response.

2.2. *Event selection*

The CMS-EXO-17-015 event selection strategy includes two stages, namely a preselection and the definition of a signal region that we coin, in the following, `SignalRegion`.

In the preselection procedure, events are first selected by requiring the presence of at least one tightly isolated muon with $p_T > 60$ GeV and $|\eta| < 2.4$. The leading jet is then required to satisfy $p_T > 100$ GeV and to be separated from the leading muon in the transverse plane by $\Delta R > 0.5$. Events satisfying those criteria are assumed to be compatible with the production of a leptoquark that decays into those leading jet and muon.

As a next step, several vetoes are applied to reduce the contamination of the overwhelming $t\bar{t}$, $W+$ jets and $Z+$ jets backgrounds. First, events are vetoed if at least one b-tagged jet is present. Moreover, a veto on events featuring either a loose electron candidate or a hadronic tau candidate is applied. These three vetoes are necessary to jointly suppress the $t\bar{t}$ background, while the electron and tau vetoes specifically suppress the $W/Z+$ jets contributions.

Next, the transverse mass (m_T) of the system comprised of the leading muon and the missing momentum is used to further suppress the $W+$ jets background: One imposes that $m_T > 100$ GeV. In addition, the contribution of the $Z+$ jets background is further reduced by rejecting events that contain one extra loosely identified muon candidate with an electric charge that is opposite to the one of the leading muon, and for which

$$|m_{\mu\mu} - M_Z| < 10 \text{ GeV}. \tag{8}$$

In this expression, $m_{\mu\mu}$ stands for the invariant mass of the system comprised of this muon and the leading muon, such a system being thus constrained to be incompatible with the decay of an on-shell Z-boson, if present in the event final state.

Finally, the preselection ends by an extra requirement on the missing momentum $\vec{p}_{\rm miss}$ that is enforced to be well separated in azimuth from the leading jet and the leading muon. We require

$$\Delta\phi(\text{jet}, \vec{p}_{\rm miss}) > 0.5 \text{ and } \Delta\phi(\mu, \vec{p}_{\rm miss}) > 0.5, \tag{9}$$

Table 1. Selection cuts defining the unique CMS-EXO-17-015 signal region. The first column introduces our naming scheme for each cut, as used in the cut-flow tables presented in the next section.

Basic requirements	
`SignalMuon`	At least one isolated muon with $p_T > 60$ GeV and $\|\eta\| < 2.4$.
`SignalJet`	The leading jet should fulfil $p_T > 100$ GeV, $\|\eta\| < 2.4$ and be separated by $\Delta R > 0.5$ from the leading muon.
Vetoes	
b-`Veto`	Veto of events featuring at least one b-jet with $p_T > 30$ GeV and $\|\eta\| < 2.4$.
tau-`Veto`	Veto of events featuring at least one hadronic tau with $p_T > 20$ GeV and $\|\eta\| < 2.3$.
e-`Veto`	Veto of events featuring at least one loosely reconstructed electron with $p_T > 15$ GeV and $\|\eta\| < 2.4$.
Further preselection requirements	
`ZMassWindow`	No extra loose muon that could arise, together with the leading muon, from a Z-boson decay (*i.e.* if $\|m_{\mu\mu} - M_Z\| < 10$ GeV).
$\vec{p}_{\rm miss}$-`threshold`	$\|\vec{p}_{\rm miss}\| > 100$ GeV.
m_T-`threshold`	The transverse mass of the muon-$\vec{p}_{\rm miss}$ system must fulfil $m_T > 100$ GeV.
Signal region	
`SignalRegion`	Extra m_T requirement: $m_T > 500$ GeV.

with $\Delta\phi(i,j) = |\phi_i - \phi_j|$. Whereas these last requirements have very minor effects on the considered signal, they allow in particular for the suppression of the multijet background. For this reason, while implemented in our recasting code, they will be absent from the cut-flow tables presented in the next section.

After this preselection, the signal region is defined by a more stringent cut on the m_T variable,

$$m_T > 500 \text{ GeV}. \tag{10}$$

A summary of the full set of selection cuts is presented in Table 1.

3. Validation

3.1. *Event generation*

For the validation of our re-implementation of the CMS-EXO-17-015 analysis, we generate events describing the dynamics of the signal of Fig. 1 in the context of the model introduced in Sec. 1. We use MadGraph5_aMC@NLO [44] to simulate hard-scattering events at the leading order (LO) in the strong coupling, excluding the potentially relevant t-channel leptonic exchange diagrams [45]. In our procedure, we convolute the LO matrix elements with the LO set of NNPDF 3.0 parton distribution functions in the four-flavour-number scheme, and with $\alpha_s(M_Z) = 0.130$. Moreover, we set the renormalisation and factorisation scales to the average transverse mass of the final-state objects.

Table 2. Cut-flow charts associated with the CMS-EXO-17-015 analysis and the process depicted in Fig. 1 for the two benchmark scenarios `BP1` (upper panel) and `BP2` (lower panel). We show results obtained with MadAnalysis 5 (second column) and those provided by the CMS collaboration (third column). The numbers inside brackets correspond to the selection efficiency of each cut and the ratio $\mathcal{R}_i$ depicting the differences between our predictions and the official CMS results is defined in Eq. (12).

Cut	MadAnalysis 5	CMS	$\mathcal{R}_i$
Initial events	99977 (100%)	99977 (100%)	0
`SignalMuon`	88583 (88.66%)	90104 (90.12%)	1.61×10^{-2}
`SignalJet`	85594 (96.62%)	88100 (97.77%)	1.17×10^{-2}
b-`Veto`	79367 (92.72%)	84282 (95.66%)	3.07×10^{-2}
τ_h-`Veto`	75572 (95.21%)	83373 (98.92%)	3.75×10^{-2}
e-`Veto`	75534 (99.94%)	83175 (99.7%)	2.41×10^{-3}
`ZMassWindow`	71795 (95.05%)	81344 (97.79%)	2.80×10^{-2}
$\vec{p}_{\rm miss}$-`threshold`	69957 (97.44%)	78665 (96.71%)	1.71×10^{-2}
m_T-`threshold`	65957 (94.29%)	74796 (95.08%)	8.30×10^{-3}
`SignalRegion`	51151 (77.75%)	54849 (73.33%)	6.02×10^{-2}

Cut	MadAnalysis 5	CMS	$\mathcal{R}_i$
Initial events	3996 (100%)	3996 (100%)	0
`SignalMuon`	3519 (88.07%)	3625 (90.71%)	2.90×10^{-2}
`SignalJet`	3441 (97.80%)	3586 (98.92%)	1.12×10^{-2}
b-`Veto`	3185 (92.57%)	3433 (95.73%)	3.33×10^{-2}
τ_h-`Veto`	3026 (95.01%)	3401 (99.06%)	4.08×10^{-2}
e-`Veto`	3024 (99.93%)	3392 (99.73%)	2.06×10^{-3}
`ZMassWindow`	2936 (97.11%)	3327 (98.08%)	9.88×10^{-3}
$\vec{p}_{\rm miss}$-`threshold`	2897 (98.69%)	3277 (98.49%)	2.07×10^{-3}
m_T-`threshold`	2678 (92.44%)	3160 (96.42%)	4.12×10^{-2}
`SignalRegion`	2162 (80.74%)	2611 (82.62%)	2.27×10^{-2}

We use Pythia 8 (version 8.432) [46] to match the fixed-order results with parton showers and to deal with the hadronisation of the resulting partons, after ignoring multi-parton interactions. The response of the CMS detector is then modeled by means of the fast detector simulation toolkit Delphes 3 (version 3.4.2) [47], that internally relies on FastJet (version 3.3.0) [48] for jet clustering. In this last step, we have designed a customized Delphes 3 parametrisation that accurately matches the actual CMS performance working points of the analysis. This card is available, together with our code, from the MadAnalysis 5 Physics Analysis Database (PAD)[b].

For the results presented in the rest of this contribution, we have generated

[b]See the webpage http://madanalysis.irmp.ucl.ac.be/wiki/PublicAnalysisDatabase.

200,000 events for two benchmark points `BP1` and `BP2` defined by

$$\begin{aligned} \texttt{BP1}: &\quad M_{\rm LQ} = 1000 \text{ GeV}, \text{ and } \quad m_\chi = 400 \text{ GeV}, \\ \texttt{BP2}: &\quad M_{\rm LQ} = 1500 \text{ GeV}, \text{ and } \quad m_\chi = 600 \text{ GeV}, \end{aligned} \tag{11}$$

with the other parameters fixed as in Eq. (3). About 102,326 (108,208) events pass all the selection criteria of the CMS analysis in the framework of the `BP1` (`BP2`) scenario.

3.2. *Results*

In order to validate our re-implementation, we compare predictions obtained with our implementation in MadAnalysis 5 to the official results provided by the CMS collaboration for the two benchmark scenarios `BP1` and `BP2` defined in Sec. 3.1. Our comparison is performed in two stages. First, we study the resulting cut-flow tables. Next, we investigate the shape of the distributions of several key observables.

To quantify the level of agreement between our results and the CMS ones at each selection step of the cut-flow, we introduce a quantity $\mathcal{R}_i$ defined by

$$\mathcal{R} = \left| 1 - \frac{\epsilon^i_{MA5}}{\epsilon^i_{CMS}} \right|, \tag{12}$$

with ϵ^i being the selection efficiency of the $i^{\rm th}$ cut i,

$$\epsilon^i = \frac{n^i}{n^{i-1}}. \tag{13}$$

In this notation, n_{i-1} events survive before the $i^{\rm th}$ cut, and n_i events survive after this cut. We present the results in the two panels of table 2 for the `BP1` and `BP2` setup respectively, after normalising our results to the same cross section as the one used by the CMS collaboration in their analysis. We obtain an excellent level of agreement, reaching $\mathcal{R} \sim 10^{-3} - 10^{-2}$.

Moreover, we confront results at the differential level in Fig. 2 for different observables relevant for the considered analysis. An excellent agreement is again found.

4. Conclusions

In this note, we have made a detailed description of our re-implementation of the CMS-EXO-17-015 analysis in the MadAnalysis 5 framework. This analysis can be used in particular to constrain models containing scalar or vector leptoquarks that decay primarily into muons and jets. However, the signal region is not defined by relying on the leptoquark invariant mass (to be reconstructed from the leading muon and jet), so that the analysis can in fact be used to probe any model giving rise to muons, jets and missing transverse energy. For given benchmark scenarios, we have found an excellent agreement between our predictions with MadAnalysis 5 and the official results provided by the CMS collaboration. This validated

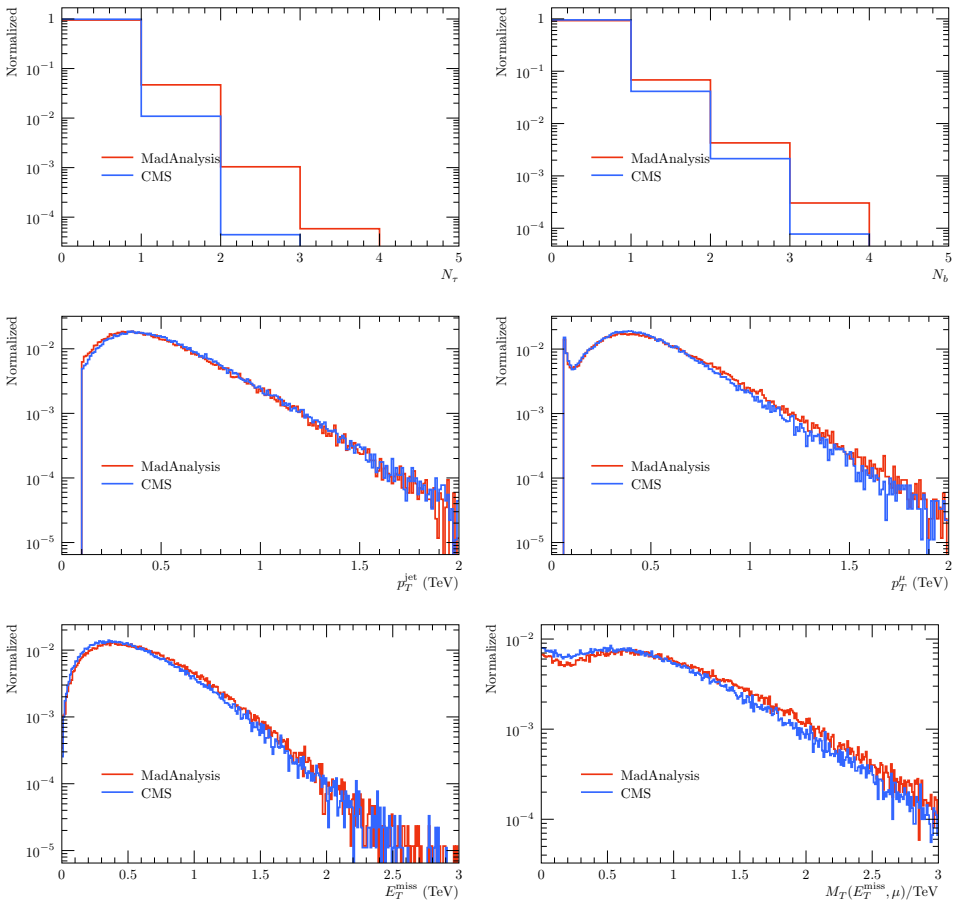

Fig. 2. Normalised distributions for some key kinematical quantities used in the CMS-EXO-17-015 analysis. We show predictions for the scenario `BP1` with $M_{\rm LQ} = 1000$ GeV. The MadAnalysis 5 predictions are shown in red while the CMS ones are given in blue. We consider the hadronic tau multiplicity (upper left), the b-jet multiplicity (upper right), the transverse momentum of the leading jet (centre left), the transverse momentum of the leading muon (centre right), the missing transverse energy (lower left) and the transverse mass of the leading muon and missing momentum system (lower right).

analysis is available on the public MadAnalysis 5 database and can be found from the MadAnalysis 5 dataverse, at https://doi.org/10.14428/DVN/ICOXG9 [49], together with relevant validation material.

Acknowledgments

The authors would like to thank Abdollah Mohammadi for kindly providing official CMS cut-flow tables and for his assistance in understanding the event selection used in the CMS-EXO-17-015 analysis. The work of AJ is sponsored by the National

Research Foundation of Korea, Grant No. NRF-2019R1A2C1009419.

References

1. J. L. Feng, S. Su and F. Takayama, *Phys. Rev. Lett.* **96**, 151802 (2006), arXiv:hep-ph/0503117.
2. A. Birkedal, K. Matchev and M. Perelstein, *Phys. Rev. D* **70**, 077701 (2004), arXiv:hep-ph/0403004.
3. Y. Bai, P. J. Fox and R. Harnik, *JHEP* **12**, 048 (2010), arXiv:1005.3797 [hep-ph].
4. P. J. Fox, R. Harnik, J. Kopp and Y. Tsai, *Phys. Rev. D* **84**, 014028 (2011), arXiv:1103.0240 [hep-ph].
5. N. F. Bell, J. B. Dent, A. J. Galea, T. D. Jacques, L. M. Krauss and T. J. Weiler, *Phys. Rev. D* **86**, 096011 (2012), arXiv:1209.0231 [hep-ph].
6. A. A. Petrov and W. Shepherd, *Phys. Lett. B* **730**, 178 (2014), arXiv:1311.1511 [hep-ph].
7. Y. Bai and T. M. Tait, *Phys. Lett. B* **723**, 384 (2013), arXiv:1208.4361 [hep-ph].
8. J. Andrea, B. Fuks and F. Maltoni, *Phys. Rev. D* **84**, 074025 (2011), arXiv:1106.6199 [hep-ph].
9. ATLAS Collaboration, M. Aaboud *et al.*, *JHEP* **06**, 059 (2016), arXiv:1604.01306 [hep-ex].
10. ATLAS Collaboration, M. Aaboud *et al.*, *Phys. Rev. D* **94**, 032005 (2016), arXiv:1604.07773 [hep-ex].
11. ATLAS Collaboration, M. Aaboud *et al.*, *Phys. Lett. B* **763**, 251 (2016), arXiv:1608.02372 [hep-ex].
12. ATLAS Collaboration, M. Aaboud *et al.*, *Phys. Lett. B* **765**, 11 (2017), arXiv:1609.04572 [hep-ex].
13. ATLAS Collaboration, M. Aaboud *et al.*, *Eur. Phys. J. C* **77**, 393 (2017), arXiv:1704.03848 [hep-ex].
14. ATLAS Collaboration, M. Aaboud *et al.*, *Phys. Rev. D* **96**, 112004 (2017), arXiv:1706.03948 [hep-ex].
15. ATLAS Collaboration, M. Aaboud *et al.*, *Phys. Rev. Lett.* **119**, 181804 (2017), arXiv:1707.01302 [hep-ex].
16. ATLAS Collaboration, M. Aaboud *et al.*, *Phys. Lett. B* **776**, 318 (2018), arXiv:1708.09624 [hep-ex].
17. ATLAS Collaboration, M. Aaboud *et al.*, *Eur. Phys. J. C* **78**, 18 (2018), arXiv:1710.11412 [hep-ex].
18. ATLAS Collaboration, M. Aaboud *et al.*, *JHEP* **01**, 126 (2018), arXiv:1711.03301 [hep-ex].
19. ATLAS Collaboration, M. Aaboud *et al.*, *JHEP* **10**, 180 (2018), arXiv:1807.11471 [hep-ex].
20. CMS Collaboration, A. M. Sirunyan *et al.*, *JHEP* **07**, 014 (2017), arXiv:1703.01651 [hep-ex].
21. CMS Collaboration, A. M. Sirunyan *et al.*, *JHEP* **10**, 180 (2017), arXiv:1703.05236 [hep-ex].
22. CMS Collaboration, A. Sirunyan *et al.*, *Eur. Phys. J. C* **77**, 845 (2017), arXiv:1706.02581 [hep-ex].
23. CMS Collaboration, A. Sirunyan *et al.*, *Eur. Phys. J. C* **78**, 291 (2018), arXiv:1711.00431 [hep-ex].
24. CMS Collaboration, A. M. Sirunyan *et al.*, *Phys. Rev. D* **97**, 092005 (2018), arXiv:1712.02345 [hep-ex].

25. CMS Collaboration, A. M. Sirunyan *et al.*, *JHEP* **06**, 027 (2018), arXiv:1801.08427 [hep-ex].
26. CMS Collaboration, A. M. Sirunyan *et al.*, *JHEP* **09**, 046 (2018), arXiv:1806.04771 [hep-ex].
27. CMS Collaboration, A. M. Sirunyan *et al.*, *Phys. Rev. Lett.* **122**, 011803 (2019), arXiv:1807.06522 [hep-ex].
28. CMS Collaboration, A. M. Sirunyan *et al.*, *Eur. Phys. J. C* **79**, 280 (2019), arXiv:1811.06562 [hep-ex].
29. CMS Collaboration, A. M. Sirunyan *et al.*, *JHEP* **03**, 141 (2019), arXiv:1901.01553 [hep-ex].
30. CMS Collaboration, A. M. Sirunyan *et al.*, *JHEP* **03**, 025 (2020), arXiv:1908.01713 [hep-ex].
31. CMS Collaboration, A. M. Sirunyan *et al.* (8 2020), arXiv:2008.04735 [hep-ex].
32. M. J. Baker *et al.*, *JHEP* **12**, 120 (2015), arXiv:1510.03434 [hep-ph].
33. CMS Collaboration, A. M. Sirunyan *et al.*, *Phys. Lett. B* **795**, 76 (2019), arXiv:1811.10151 [hep-ex].
34. E. Conte, B. Fuks and G. Serret, *Comput. Phys. Commun.* **184**, 222 (2013), arXiv:1206.1599 [hep-ph].
35. E. Conte, B. Dumont, B. Fuks and C. Wymant, *Eur. Phys. J. C* **74**, 3103 (2014), arXiv:1405.3982 [hep-ph].
36. B. Dumont, B. Fuks, S. Kraml, S. Bein, G. Chalons, E. Conte, S. Kulkarni, D. Sengupta and C. Wymant, *Eur. Phys. J. C* **75**, 56 (2015), arXiv:1407.3278 [hep-ph].
37. E. Conte and B. Fuks, *Int. J. Mod. Phys. A* **33**, 1830027 (2018), arXiv:1808.00480 [hep-ph].
38. J. Y. Araz, M. Frank and B. Fuks, *Eur. Phys. J. C* **80**, 531 (2020), arXiv:1910.11418 [hep-ph].
39. CMS Collaboration, A. Sirunyan *et al.*, *JINST* **13**, P06015 (2018), arXiv:1804.04528 [physics.ins-det].
40. CMS Collaboration, V. Khachatryan *et al.*, *JINST* **10**, P06005 (2015), arXiv:1502.02701 [physics.ins-det].
41. CMS Collaboration, A. Sirunyan *et al.*, *JINST* **13**, P10005 (2018), arXiv:1809.02816 [hep-ex].
42. M. Cacciari, G. P. Salam and G. Soyez, *JHEP* **04**, 063 (2008), arXiv:0802.1189 [hep-ph].
43. CMS Collaboration, A. Sirunyan *et al.*, *JINST* **13**, P05011 (2018), arXiv:1712.07158 [physics.ins-det].
44. J. Alwall, R. Frederix, S. Frixione, V. Hirschi, F. Maltoni, O. Mattelaer, H. S. Shao, T. Stelzer, P. Torrielli and M. Zaro, *JHEP* **07**, 079 (2014), arXiv:1405.0301 [hep-ph].
45. C. Borschensky, B. Fuks, A. Kulesza and D. Schwartländer, *Phys. Rev. D* **101**, 115017 (2020), arXiv:2002.08971 [hep-ph].
46. T. Sjöstrand, S. Ask, J. R. Christiansen, R. Corke, N. Desai, P. Ilten, S. Mrenna, S. Prestel, C. O. Rasmussen and P. Z. Skands, *Comput. Phys. Commun.* **191**, 159 (2015), arXiv:1410.3012 [hep-ph].
47. DELPHES 3 Collaboration, J. de Favereau, C. Delaere, P. Demin, A. Giammanco, V. Lemaître, A. Mertens and M. Selvaggi, *JHEP* **02**, 057 (2014), arXiv:1307.6346 [hep-ex].
48. M. Cacciari, G. P. Salam and G. Soyez, *Eur. Phys. J. C* **72**, 1896 (2012), arXiv:1111.6097 [hep-ph].
49. B. Fuks and A. Jueid, *https://doi.org/10.14428/DVN/ICOXG9* (2020).